Identifying Damage on a Bridge Using Rotation – Based Bridge Weigh – In – Motion

E.J. OBrien[1], J.M.W. Brownjohn[2,3], D. Hester[4], F. Huseynov[5], M. Casero[1]

[1] School of Civil Engineering, University College Dublin, Newstead, Belfield, Dublin, D04 V1W8, Ireland

[2] Vibration Engineering Section, College of Engineering, Mathematics and Physical Sciences, University of Exeter, North Park Road, EX4 4QF Exeter, UK

[3] Full Scale Dynamics LTD, Kay Building North Park Road, EX4 4QF Exeter, UK.

[4] School of Natural and Built Environment, Queen's University Belfast, Stranmillis Road, BT9 5AG Belfast, Northern Ireland, UK.

[5] Department of Engineering, University of Cambridge, CB2 1PZ, Cambridge, UK

Contact author: Farhad Huseynov
University of Cambridge
Department of Engineering
Trumpington Street
Cambridge. UK
CB2 1PZ
E-mail: ferhad_huseynov@yahoo.com
Tel: +447533118686

Body text word count: 5205
Number of figures: 12
Number of tables: 2

Abstract

Bridge Weigh-In-Motion (B-WIM) systems use the bridge response under a traversing vehicle to estimate its axle weights. The information obtained from B-WIM systems has been used for a wide range of applications such as pre-selection for weight enforcement, traffic management/planning and for bridge and pavement design. However, it is less often used for bridge condition assessment purposes which is the main focus of this study. This paper presents a bridge damage detection concept using information provided by B-WIM systems. However, conventional B-WIM systems use strain measurements which are not sensitive to local damage. In this paper the authors present a B-WIM formulation that uses rotation measurements obtained at the bridge supports. There is a linear relationship between support rotation and axle weight and, unlike strain, rotation is sensitive to damage anywhere in the bridge. Initially, the sensitivity of rotation to damage is investigated using a hypothetical simply supported bridge model. Having seen that rotation is damage-sensitive, the influence of bridge damage on weight predictions is analysed. It is shown that if damage occurs, a rotation-based B-WIM system will continuously overestimate the weight of traversing vehicles. Finally, the statistical repeatability of ambient traffic is studied using real traffic data obtained from a Weigh-in-Motion site in the U.S. under the Federal Highway Administration's Long Term Pavement Performance programme and a damage indicator is proposed as the change in the mean weights of ambient traffic data. To test the robustness of the proposed damage detection methodology numerical analysis are carried out on a simply supported bridge model and results are presented within the scope of this study.

Keywords:

 Bridge, damage detection, rotation, Bridge Weigh-in-Motion, B-WIM, WIM, ambient traffic.

1 Introduction

While the bridge stock around the world is ageing, freight transport is growing and the demand on transport infrastructure is therefore increasing. Bridges are typically designed to maintain their functionality for 75 to 100 years of service life. A recent survey of European's highway infrastructure has revealed that almost half of Europe's bridges were built before the 1960s and have now exceeded their planned service life [1]. During this period, they were subject to degradation processes due to environmental and loading conditions. Therefore, accurate bridge condition assessment methods are needed to verify the safety of older structures.

In the simplest term, SHM systems can be categorised in four levels based on the type of information they are capable of providing [2]. These four levels are as follows:

Level I: Identifying the presence of damage.

Level II: Detecting the presence of damage and its location.

Level III: Quantifying the severity of damage and its location.

Level IV: Quantifying the reserve capacity of the structure.

A new Level I bridge condition assessment method is proposed in this paper that uses a Bridge Weigh-in-Motion (B-WIM) algorithm. A conventional B-WIM system is designed to estimate the axle weights of vehicles traversing a bridge structure. It typically consists of sensing equipment, traditionally strain transducers [3], [4], to record bridge deformations and identify the vehicle's speed and axle spacings. While traditionally strains have been used as the main parameter in the B-WIM systems more recently authors have proposed using displacement [5] and rotation [6] measurements. In this paper, rotation is measured at the support as it is sensitive to bridge damage away

from the sensor location. The concept is that a change in the population of inferred vehicle weights is an indication that the bridge is damaged.

The B-WIM algorithm first proposed by Moses [7], which forms the basis of most installed B-WIM systems, is based on the use of influence lines (IL's). The IL's of a structure are typically obtained during installation by measuring the responses to a vehicle with known axle weights and spacings. Once calibrated in this way, the system finds the axle weights of passing vehicles by best fitting measurements to the corresponding theoretical responses. The formulations used in B-WIM system are further explained in the following sections. B-WIM technology is mostly used for road bridges; however in recent studies it has also been successfully applied to a railway bridge [8]–[10].

Weigh-In-Motion systems were initially developed for overload monitoring and control purposes. However data gathered from WIM systems has also been used for other purposes such as updating notional traffic load models for bridge design [11], developing a site-specific bridge load model [12], calculating a dynamic amplification factor for bridge design and/or assessment [13], planning and management of road infrastructure [14], and assessment of fatigue load calculations [15]–[17]. In recent studies, it has also been investigated for SHM purposes. Cantero and Gonzalez propose a new damage detection method using combined information provided by pavement-based and bridge-based WIM systems [18]. It has been shown numerically that when damage occurs, a B-WIM system miscalculates the weight of the traversing vehicle, whereas the pavement based WIM system, which is not sensitive to bridge damage, estimates vehicle loads without bias. In this study, a damage indicator is defined as the relative difference in gross vehicle weight inferred by the two systems. In [19] the authors introduce a fictitious weightless axle, termed a Virtual Axle, in the Weigh-In-Motion algorithm to derive a damage indicator. In essence, if damage occurs then the

B-WIM algorithm overestimates the weight of the virtual axle. In another study, data obtained from a B-WIM system is used as input to an artificial neural network to evaluate the condition of a bridge [20]. After a learning phase, this system is able to detect the occurrence of damage by predicting the bridge response and comparing it with the measurements. It is of note that, in all of these studies, the use of B-WIM technology for SHM purposes is limited to integral bridges. This is because the B-WIM systems investigated in these studies use strain sensors to measure bridge deformations, which are only sensitive to local damage at the sensor location in a statically determinate structure. However, to make B-WIM SHM applicable for other bridge types (e.g. simply-supported bridges) it makes more sense to use displacement – or rotation – based B-WIM for damage detection. Fortunately, while conventional B-WIM systems use strain measurements, the concept has also been successfully applied using deflection [5] and rotation measurements [6], which are sensitive to damage remote from the sensor location [21].

This paper proposes a novel approach of using rotation-based Bridge Weigh-in-Motion for damage detection. Broadly speaking, in the proposed method, damage is manifested as an increase in the rotation signals measured at the bridge supports during the crossing of a typical vehicle. However, rather than looking directly at rotation values which are subject to natural variations, in this paper the rotation measurements are used in a B-WIM algorithm to predict the axle weights of the passing vehicles. If damage occurs, the system will show an increase in the inferred weight. Unlike directly measured rotation where the 'healthy-bridge answer' is unknown, when working with a traffic population, the healthy-bridge answer can be found – it is the statistical distribution of vehicle weight data for the site.

A B-WIM algorithm using rotation measurements is outlined in Section 2, along with the effect of damage on inferred axle weights. In Section 3, the statistical repeatability

of ambient traffic data obtained from a WIM site in the U.S. is investigated. Finally, capability of the proposed method to detect local damage on a bridge structure is demonstrated through numerical analysis on a 3-D FE bridge model.

2   Influence of damage on B-WIM results

This section develops the theoretical basis for the proposed approach. Section 2.1 describes how B-WIM can be implemented using rotation data measured at the end of a bridge deck; Section 2.2 shows how damage will affect the magnitude of this rotation and Section 2.3 looks specifically at the effect of damage on the predicted load.

2.1   Bridge weigh-in-motion using rotation

Unlike strain in a determinate structure, rotation is influenced by the stiffness in all parts of a bridge deck. Hence, in principle, no matter where the damage is, it will have some effect on the rotation measurement.

B-WIM can be implemented for any measurable quantity that is a function of traffic load. Here, a B-WIM algorithm is presented where rotation is the measured quantity. This formulation follows the same principles as B-WIM using strain and, as such, is based on Moses' algorithm [7]. Total (static) rotation at an instant in time, due to a moving vehicle, can be calculated by combining the contributions of each axle on the bridge. This results in a system of equations defining the rotation time history:

$$[\theta^{\mathrm{T}}]_{\mathrm{K}\times 1} = [\mathrm{IL}]_{\mathrm{K}\times \mathrm{N}} \times [\mathrm{P}]_{\mathrm{N}\times 1} \qquad (1)$$

where $[\theta^{\mathrm{T}}]$ is a vector comprising of total theoretical rotation values, [IL] is a matrix containing influence line ordinates for each axle and each instant in time, [P] is the vector of axle weights, K is the total number of sampling points (scans) and N is the number of axles.

In reality, the response of a structure to a moving load consists of not only static but also dynamic components which oscillate about the static response. Typically, it takes about a second for a vehicle travelling at a highway speed limit to cross a short- to

7

medium-span bridge. Given that the measurements during a vehicle pass are recorded at a high sampling frequency (e.g. 256 Hz) and the time history data contains many data points, Moses proposed an error function, E, defined in Eq. (2) as the sum of squares of differences between the measured and theoretical responses, to smooth out the dynamic components.

$$E = \sum_{k=1}^{K}[\theta_k^M - \theta_k^T]^2 \qquad (2)$$

where k is the scan number and $\theta_k{}^M$ is the measured rotation (including both static and dynamic components) at scan k.

Eq. 1 is substituted into Eq. 2 and the error function is minimised with respect to individual axle weights, P_i, by setting partial derivatives to zero. This leads to Eq. (3), which forms the basis of most current B-WIM systems:

$$[P]_{N\times 1} = \left([IL]_{K\times N}^T \times [IL]_{K\times N}\right)^{-1} \times [IL]_{K\times N}^T \times [\theta^M]_{K\times 1} \qquad (3)$$

In summary, B-WIM is an inverse type problem where deformations are measured and the axle loads causing the deformations are calculated by minimising the sum of squared differences between theory and measurement. The influence line clearly plays a central role. It describes the response of the bridge at a particular location to a unit point load passing overhead. It is a physical property dependent on the material and geometric properties as well as the boundary conditions of the structure. Since the boundary conditions of many bridges lie between ideal simply supported and fully fixed, the true IL of the structure should be determined during the calibration process before any B-WIM system becomes operational. In practice, the IL of a structure is obtained from a vehicle with known axle weights and spacings passing over the bridge at a known traffic speed [22]. Once the influence line for a structure is known, then the [IL] matrix can be

formed for any vehicle based on its axle configuration and speed, and axle weights can be calculated by applying Eq. (3).

The approach of B-WIM using rotation can be applied to any type of bridge structure. As a general rule, inclinometers or other rotation measuring devices, should be placed at locations where the magnitude of measurements is greatest as this maximises the signal to noise ratio. For strain or deflection based B-WIM systems, measurements are usually at mid-span. For the rotation based B-WIM on the other hand, the sensors for simply supported bridge structures are best located at one or both supports. In this section, the feasibility of using the B-WIM system for damage detection method is demonstrated using numerical simulations of a simply supported bridge. The Finite Element (FE) model used for the simulations is shown in Fig. 1 (a). Hypothetical inclinometers are placed at support locations on both sides.

2.2   Sensitivity of Rotation to Damage

Based on the Moment-Area theorem, the change in rotation between any two points along the length of the structure is equal to the corresponding area under the curvature or M/EI diagram, where M is moment. It follows that if there is a change in structural stiffness, EI, either globally or locally, at any location along the length of the structure, a change in rotation will result. This is illustrated in Figure 1, which shows the rotational responses at the ends of a 20 m long simply supported bridge to the passage of a 2-axle truck.
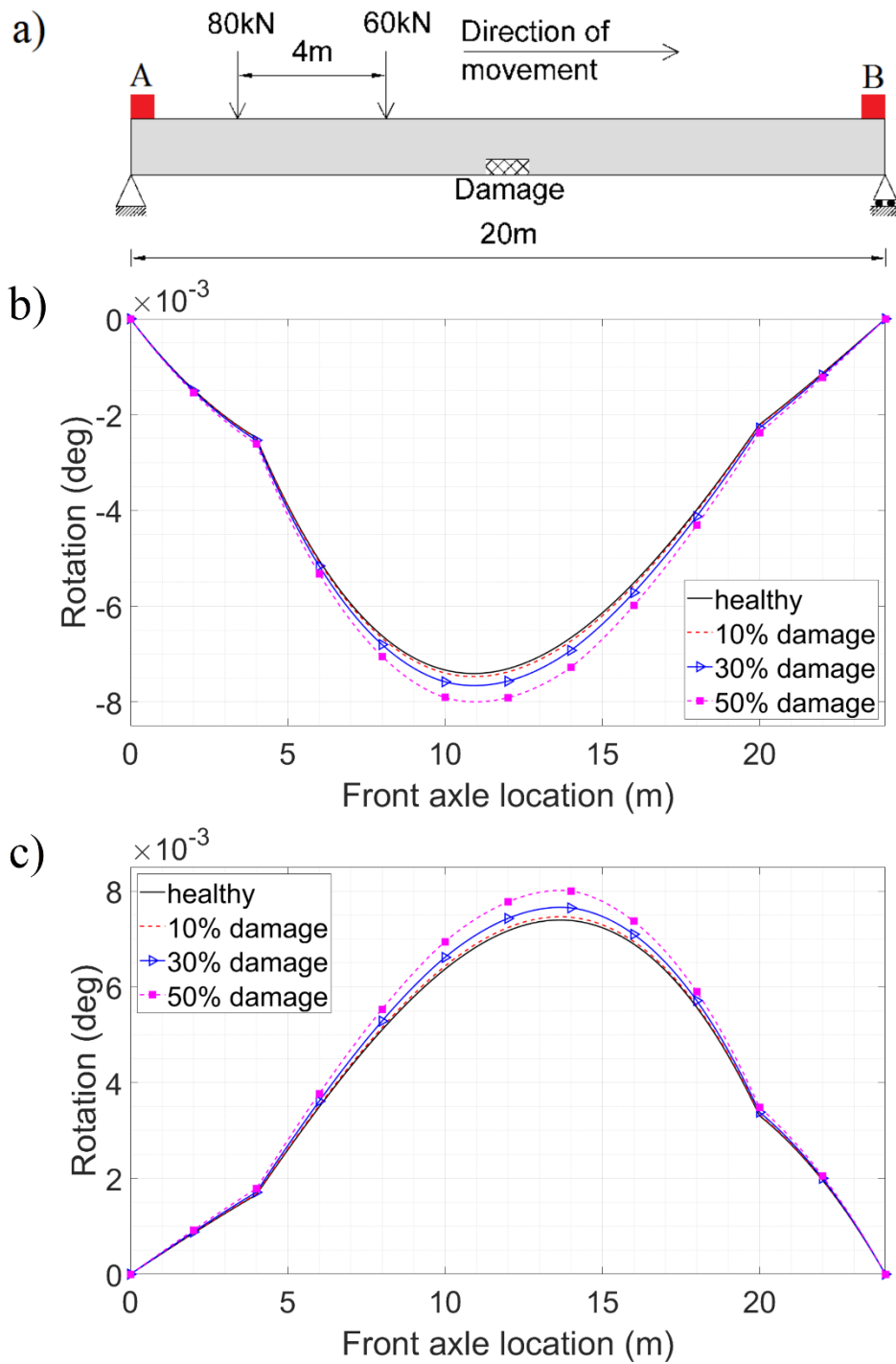
Figure 1. Effect of damage on the rotation experienced in a simply supported bridge, a) sketch of a hypothetical bridge under 2 axle moving load. b) Rotation recorded at point A c) Rotation recorded at point B.

The flexural properties of the bridge are those of a structure 10 m wide with 9 No Y3 precast concrete beams spaced at 1.25 m centres joined by a 160 mm thick deck slab [23]. This gives a total depth of 1060 mm and a second moment of area of 0.76 m^4 and a total cross sectional area of 5.2 m^2. Young's modulus is taken as 35 GPa. The moving vehicle has front and rear axle weights of 60 kN and 80 kN respectively, spaced 4 m apart. Damage is modelled as a local reduction in stiffness over 1 m (5% of the bridge length) at mid-span with various levels of severity: 10%, 30% and 50%.

Figure 1(a) is the bridge elevation while Figures 1 (b) and (c) show the rotation "recorded" at inclinometers placed at the left and right hand supports, respectively as the vehicle passes the healthy and damaged bridges. Discontinuities can be seen as axles arrive on and leave the bridge and the rotations are clearly greater for the damaged cases. The magnitude of rotations obtained from the numerical model is around 8×10^{-3} degrees which is feasible to measure using the state-of-art sensors. In the last decade, the performance and accuracy of inclinometers have been significantly improved, and it is now possible to measure inclinations to a microradian (10^{-6} radians) accuracy [24]–[27]. An in-depth investigation of the sensitivity of rotation measurements to damage is presented in [28].

To show that rotation measurement is feasible on real bridges, Figure 2 shows field measurements for a 4-axle truck crossing a bridge that spans 17.28 m over a canal. The bridge is a lifting bascule bridge, but once in the down position, the bridge effectively behaves as simply supported. These responses were measured using two uniaxial Honeywell QA-750 accelerometers, which were placed at each support locations. Recent works examined the attributes of these sensors in the context of SHM applications [29], [30]. One of the capabilities of these high-end DC accelerometers is that they allow measurement of the DC component of the signal with very low noise at 0 Hz in the frequency domain, i.e., they can sense gravity under quasi-static conditions.

Since the output of an accelerometer obeys a sinusoidal relationship when it is rotated through gravity, such as when it is pointed in the horizontal direction it records 0g whereas when it is placed in the vertical direction it reads +/- 1g based on the direction of axis of measurements, the conversion from acceleration to rotation could be obtained by using the inverse sine function as given in Eq. (4).

$$\theta = sin^{-1}(Acc[g]) \times \frac{\pi}{180} \qquad (4)$$

where the estimated rotation value, θ, is in degrees.

In practice, as well as experiencing rotation due to the static effects of the load, the bridge will also contain some level of dynamic response and measurement noise. This can be filtered by applying a low pass filter on the raw acceleration data.

Figure 2. Example of rotation measurements recorded in the field, a) elevation of the bridge, b) four axle 32 tonne truck used during load testing, c) Rotation time history recorded using an inclinometer placed near the left support d) Rotation time history recorded using an inclinometer placed near the right support

The accuracy of rotation measurements obtained using accelerometers has been investigated by the authors in recent studies [31]–[33]. In [31], [32], the authors instrumented a railway bridge with QA-750 accelerometers to measure rotations at five locations along the bridge span. Using this [34], they calculated the midspan deflections of the bridge deck. Calculated midspan deflections were later validated with deflections measured with an optical camera system. The comparison of deflection values obtained using rotation measurements with direct measurements (i.e. optical camera) provided some evidence of the degree of accuracy of the rotation measurements (using QA-750 accelerometers). In another study, the authors conducted extensive laboratory experiments on a bridge model to validate the robustness of a novel bridge damage detection methodology using direct rotation measurements [33]. The results showed that the rotation measurement technique described above can sense the effect of damage on the bridge model for a damage level as low as 7% change in stiffness applied over a length of 2.5% of the bridge span.

2.3   Effect of damage on predicted load

As demonstrated in the previous section, damage in a bridge structure results in higher magnitudes of rotation for a given loading. Assuming that the structure is not recalibrated after damage, then the B-WIM algorithm for the damaged case infers loads using the 'healthy' influence line but larger measured rotations (Eq. (3)):

$$[P^*]_{N \times 1} = \left([IL]^T_{K \times N} \times [IL]_{K \times N}\right)^{-1} \times [IL]^T_{K \times N} \times [\theta^{M*}]_{K \times 1} \qquad (5)$$

where $[\theta^{M*}]_{K \times 1}$ is a vector containing the measured rotations for the damaged case ($\theta^{M*} > \theta^{M}$) and $[P^*]_{N \times 1}$ is a vector consisting of the corresponding inferred axle weights. Since the [IL] matrix in the formulation remains the same as the initial (healthy) case

but the magnitudes of rotations ($\theta^{M}*$) increase due to the damage, the B-WIM algorithm will consistently overestimate the Gross Vehicle Weight (GVW).

To further investigate the effect of damage on the B-WIM analysis, numerical analysis was carried out using the bridge and vehicle models presented in Figure 1 of section 2.2. The damage was simulated at three different locations, at ¼ L, ½ L and ¾ L, as 30% loss in stiffness over a 1 m length. The rotation time history under the two axle truck was obtained from the numerical model for the healthy and damaged cases using the hypothetical inclinometer placed at the left hand support. The axle weights were then back-calculated using the healthy influence line for the healthy and damaged cases, respectively. Figure 3 shows the axle weights calculated by the algorithm for the healthy case and bridges with damage at 3 separate locations. Note the x and y axes in the figure show the calculated weights for axles 1 and 2, respectively. For the healthy case, the correct axle weights are found, i.e. 60 kN and 80 kN for axles 1 and 2 respectively, (see Figure 1). For the damaged cases axle weights are generally but not always overestimated. The error in Axle 1 weight is greater than the error in Axle 2 when damage is at ¼ span. For damage at ¾ span, the error in Axle 2 weight is greater and the Axle 1 weight error is actually slightly negative. However, the GVW estimated for all damaged bridge states are greater than the actual GVW of the simulated vehicle.
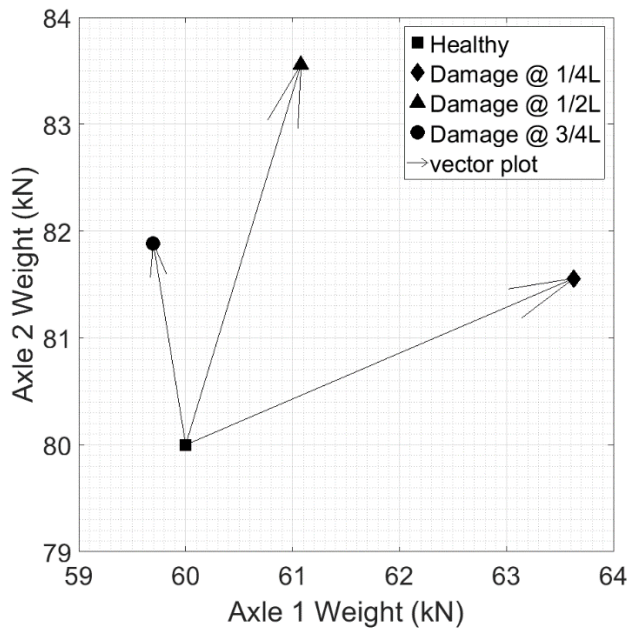
Figure 3. Vector plot of change in axle weights in W1/W2 space due to damage

Figure 3 shows vectors representing the changes in inferred axle weights due to damage in Axle 1/Axle 2 space. If there were a pavement based WIM system beside the bridge, (see, for example, [18]), then it would be relatively easy to identify damage from this plot. The relative difference in the magnitudes of the weights inferred by the two systems indicates the severity of damage and the inclination of the vector gives an indication of its location. However, WIM systems are expensive to install and are often not accurate for individual vehicle weights. Therefore, a method for inferring damage that does not require an adjacent pavement based WIM system is proposed and investigated in Sections 3 and 4.

It should be noted that the bridge influence line might also be affected by events other than local (bridge strike) damage such as bearing failure or a possible change in road surface profile due to a deteriorating pavement condition. The failure of a bearing intended to allow free rotation would have a significant effect on the whole shape of a rotation IL. While it should be possible in many cases to distinguish between bridge

strike and bearing damage, the objective in this paper is simply to detect a change which prompts further investigation.

Pavement condition is known to affect the accuracy of B-WIM so a deterioration of the pavement may affect the damage indicator. However, B-WIM systems have been in place at some sites for years without significant loss of accuracy. It is therefore not anticipated that pavement deterioration will be a particular problem in most cases.

3 Ambient traffic

While the weights of individual vehicles crossing a bridge are generally not known, there are statistical features of the population of vehicle weights at a site that are repeatable. Therefore, in this section, a population of 5-axle trucks is considered, together with the influence that bridge damage has on the population of inferred weights. Data from the U.S. Federal Highway Administration's Long-Term Pavement Performance (LTPP) programme is used for the population of trucks. Through the LTPP, data has been collected at various sites in North America since 1989. In 2001, quality control procedures were centralised and improved through a national pooled-fund study [35]. Since then "research quality" data is being collected at 19 LTPP sites in 17 different states across the U.S. The WIM technologies currently being used for traffic data collection include only bending plate, load cell, and piezo-quartz, all of which meet the research quality data standard. Results from the validation tests are presented in Table 1, which shows the accuracy level of the WIM systems instrumented under the LTPP programme.

Table 1. Accuracy of LTPP data obtained from the validations tests (95% confidence level) [35]

Parameter	Accuracy	
	Data from 2001	Data from 2005
Gross Weight	-18% to +30%	$0.2\% \pm 8.2\%$
Tandem axles	-26% to +41%	$0.0\% \pm 10.2\%$
Single Axles	-31% to +38%	$1.2\% \pm 10.0\%$

For the purpose of this study, 4 years of data (2009 - 2012) collected from Lane 2 of the Virginia site, is investigated. The average total number of vehicles at the selected site is around 393,000 per year with an average daily truck traffic in the monitored lane of 1,087. The data available to the authors had already been cleaned according to federal and state regulations and only non-permit, i.e. regular truck data, were present [36]. According to LTPP standards the vehicles are categorised into 15 classes based on their axle configurations and weight distributions. In general, excluding the lightest vehicles (GVW < 3.5 tonnes), the typical distribution of vehicle by class at the selected site is shown in Figure 4. Vehicle Class 9 is a 5-axle semi-trailer consisting of a 3-axle tractor (steer axle + tandem) and a trailer with a 2nd tandem [37]. This vehicle class was selected for further study since it is the predominant type of truck configuration at the site.
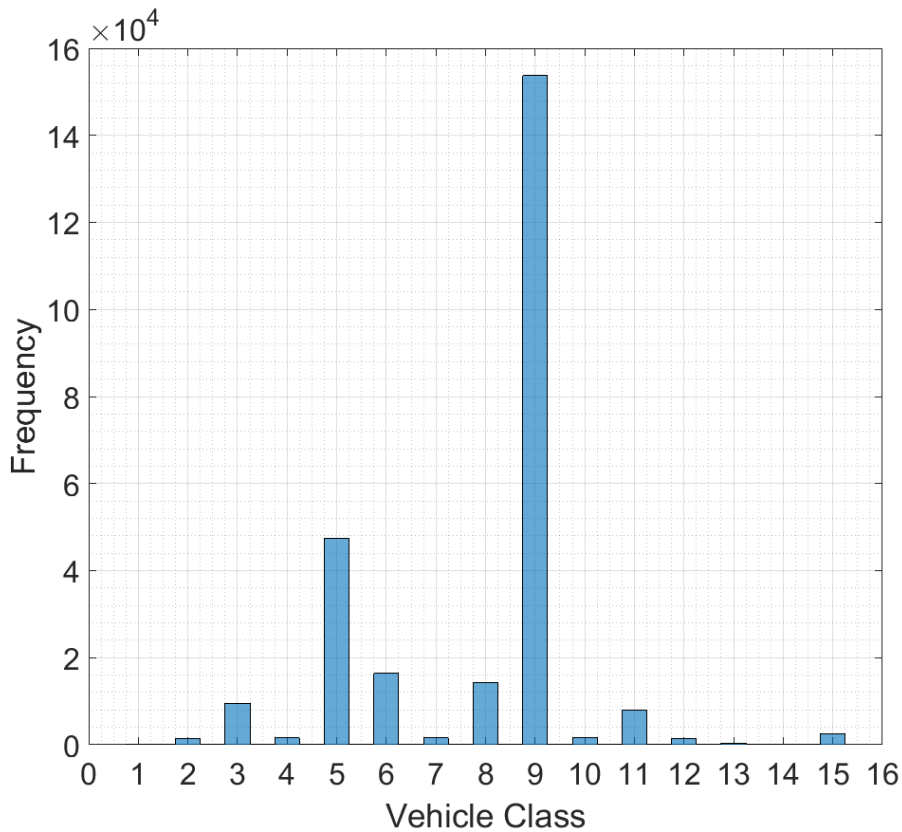

Figure 4. Histogram of vehicle Classes of traffic data collected during 2009 on Lane 2 at LTPP site in Virginia [37]

The degree of variability in the Class 9 gross weight distributions from year to year is illustrated in Figure 5. It can be seen that the peaks at around 16 tonnes and 35 tonnes, which correspond to unloaded and loaded trucks respectively, are consistent from year to year. Figure 6 shows the variability in monthly average tandem weights of loaded trucks, defined here as trucks with GVW > 30 tonnes, and the relationship between the weights of the two tandems. Tandem 1 on the tractor and tandem 2 on the trailer are plotted on the abscissa and ordinate axes, respectively. As would be expected, there is more variability in tandem weights than GVW. As Tandem 1 is part of the tractor and is influenced by engine weight as well as payload, it is less variable than Tandem 2. The dashed curve encloses the 95% confidence interval for the 48 points. The red and blue arrows in the figure represent the major and minor axes of the confidence area. These vectors indicate the directions in which the average tandem weights vary and are defined by the covariance matrix. Specifically, the arrows are the eigenvectors of the covariance matrix of the data and their lengths represent the eigenvalues. The hypothesis is that any average tandem weight combination that falls outside the 95% confidence interval is anomalous and indicates that the bridge may be damaged which would induce errors in the calculated weights. To test this, numerical simulations are carried out which are explained in detail in the following section.
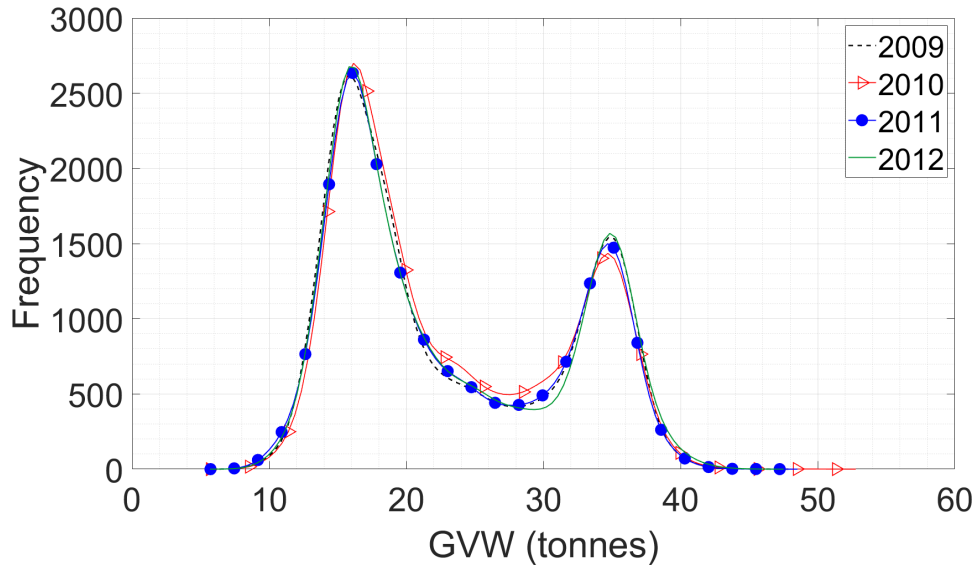
Figure 5. Repeatability of Class 9 vehicle data. Annual histograms of Gross Vehicle Weight (GVW).
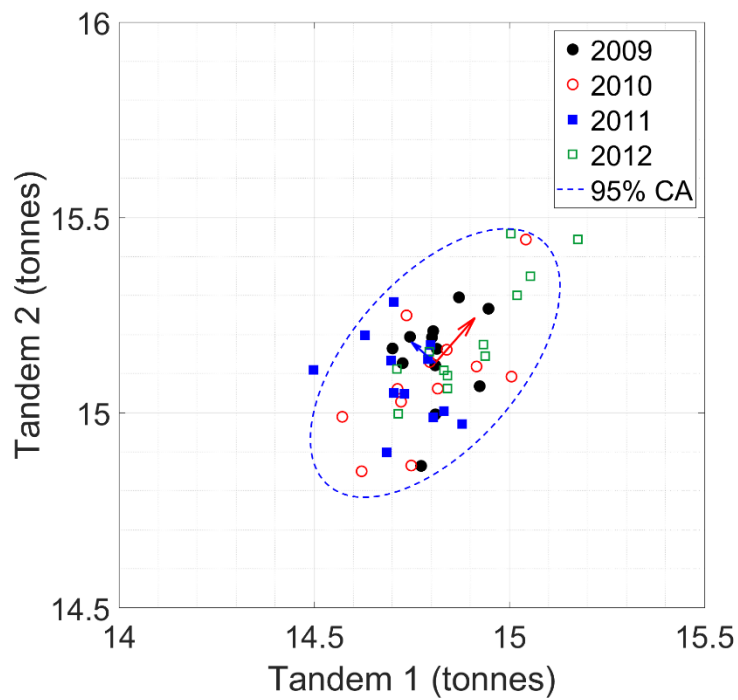

Figure 6. Monthly average tandem weights of loaded Class 9 vehicles at Virginia site (Tandem 1 in tractor; Tandem 2 in trailer). There are 12 markers in each colour, corresponding to the 12 months of that year.

4   Method Verification on a 3-D FE model

A 3-D FE bridge model is developed using Nastran Software to test the capability of the proposed bridge damage detection methodology under more realistic conditions. The hypothetical structure is modelled as a 20 m long and 11 m wide simply supported bridge, composed of a 0.2 m thick solid slab and 0.9 m deep 10 beams spaced at 1 m apart. Figure 7 shows the elevation and the cross-sectional view of the bridge model.
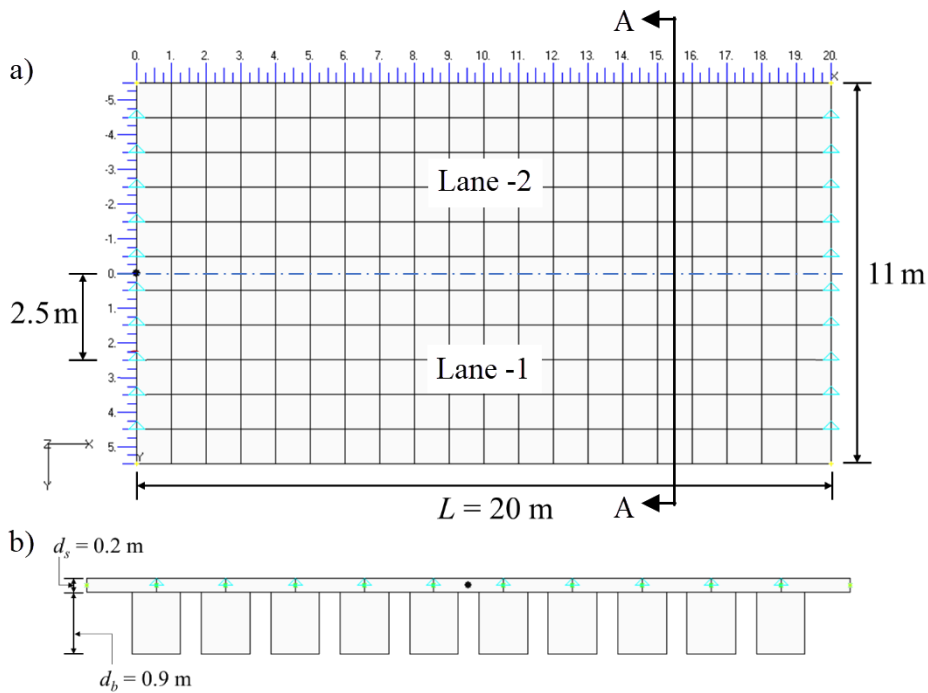

Figure 7. 3-D FE bridge model. a) Plan view b) cross-sectional view (A-A)

The slab is represented by 1m x 1 m 2-D plate elements while the beams are modelled as a series of 1-D beam elements. The modulus of elasticity for plate and beam elements are assigned as 30 GPa and 33 GPa, respectively, to simulate in situ concrete slab and precast beams. The Poisson ratio is assigned as 0.15 and the shear modulus is calculated assuming an isotropic material for all element types. The material density is set at 2500 kg/m^3 both for the slab and the beams. In order to simulate the presence of a diaphragm

at both ends of the bridge, the second moment of area of the beams is set higher for elements close to the supports in comparison to the rest of elements. As a result, the 2nd moment of area of the beam elements between $x = 1$ m and $x = 19$ m (I_b) equalled 0.0685 m^4 while in the ranges $x = [0,1]$ and $[19,20]$ m ($I_{b,supports}$) it was increased by up to 0.108 m^4.

Three damage scenarios are investigated in this study where damage is modelled at L/4, L/2 and 3L/4 span locations, one at a time. In each test scenario, damage is modelled as a reduction in the flexural stiffness of beam elements (i.e. slab elements remain intact) over three 3 m extent. At each damage location, girders consist of three elements, each 1 m long. The stiffness of the central beam element is reduced by 40% whereas the stiffnesses of the two adjacent elements are reduced by 13 %. Since the slab elements remain intact, the corresponding equivalent damage levels on the composite precast beam and "in-situ" slab section are approximately 32% and 10% for central and two adjacent damaged elements, respectively. In the transverse direction, damage is modelled along the full width of Lane – 1 (i.e. half of the bridge width).

Real traffic data obtained at the Virginia WIM site in 2009-2012 (described above) is used to simulate ambient traffic. The bridge model is loaded with the traffic population crossing along Lane-1. The hypothetical inclinometer is located at the left hand support, at the coordinate [0 m , 2.5 m] (see Figure 7) to record the rotation response of the bridge to a traversing vehicle. This is repeated for the healthy and the damaged cases and the rotation time history data obtained from the FE model is used to back-calculate the tandem axle weights of the traversing vehicles by applying Eqs. (3) and (5). The results are further elaborated in the following section.

5   Results and Discussions

Figure 8 shows the average monthly inferred tandem weights for the population of Class 9 trucks for the healthy and the 3 damaged cases (described above) calculated using the rotation signal obtained at the coordinates, [0 m, 2.5 m] (i.e. left-hand support). The circular data markers correspond to the healthy bridge while the triangular markers correspond to the damaged cases. Those months where the healthy bridge results fall outside the 95% curve are shown solid. These indicate false positives – damage is implied, but the bridge is healthy. This is because the curve is derived based on the 95% confidence area, hence some of the data remains outside of the curve. The triangular markers in the figure correspond to the damaged bridge scenarios. Open triangles are for months where the bridge is damaged and the average inferred weights confirm this to be the case, i.e., damage successfully detected. Closed triangles are for months where the bridge is damaged, but the inferred tandem weight combination falls inside the 95% curve, i.e., damaged but damage not detected.
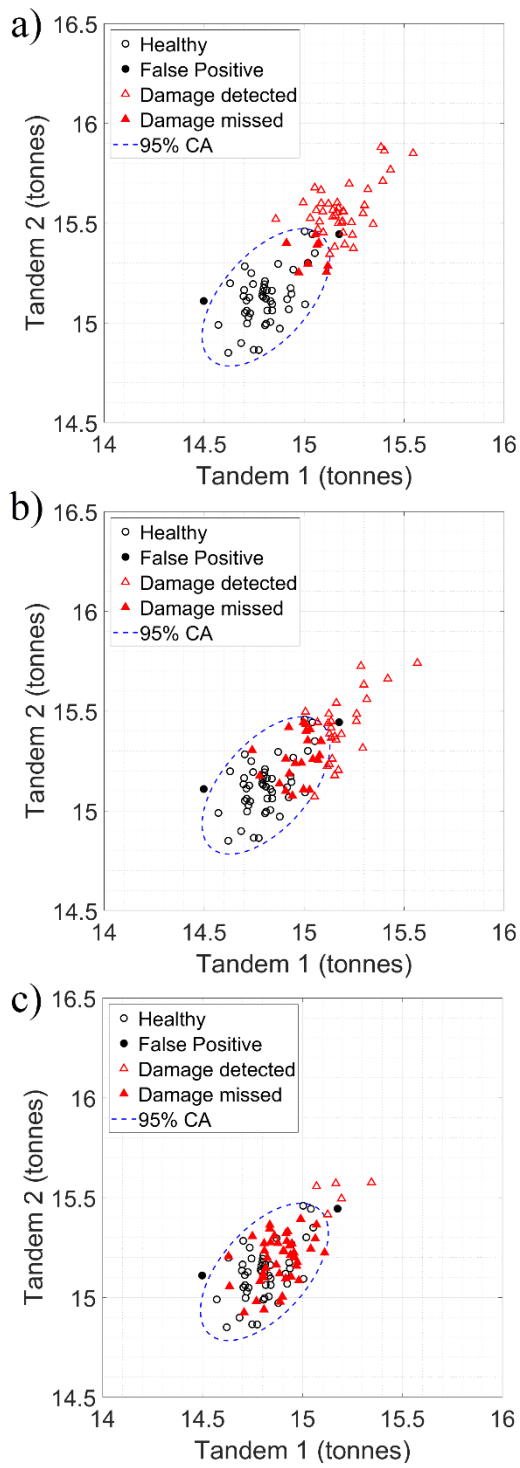
Figure 8. Monthly average tandem weights inferred from left inclinometer signals for healthy and damaged cases. a) damage at ¼ span (b) damage at ½ span c) damage at ¾ span.

The method can be seen to work well for damage at ¼ span (Figure 8 (a)), closest to the inclinometer location (i.e. left-hand support, at [0 m, 2.5 m] coordinates). There are only two false positives and seven damage-missed cases out of 48. For damage at mid-span, the number of damage-missed cases has increased to twenty (Figures 8 (b)) and for damage at ¾ span (Figure 8(c)), there is a strong overlap between the healthy and damaged populations, making it infeasible to use this as a means of detecting damage. Another conclusion from Figure 8 is that the ability of the proposed methodology to identify damage reduces as damage occurs further away from the sensor location. It should be noted that this is a pseudo-static analysis only. For bridges where there is significant dynamics, detecting damage may be more difficult.

Numerical analyses were carried out to further investigate the influence of damage location on inferred weight. An analysis similar to that mentioned above is carried out but this time the inclinometers are placed on both support locations (coordinates [0 m, 2.5 m] and [20 m , 2.5 m]). The histogram of change in GVW due to damage (inferred GVW minus true weight of a 5-axle truck) is extracted in Figure 9 using each individual inclinometer. Figures 9 (a) to (c) show the weight error histograms for damage at ¼ L, ½ L and ¾ L locations using an inclinometer placed at the left hand support. Figures 9 (d) to (f) show the corresponding histograms for an inclinometer placed at the right-hand support. The abscissa in each figure shows the observed change in the axle weight. It can be seen in the plots that the error in GVW weight, which obviously reflects the sensitivity of a sensor location to damage, reduces when the damage is further away from the sensor location. For example, in Figure 9(a) the highest frequency of error in GVW, corresponding to loaded 5 axle trucks, (second peak on the graph) is around 1.2-1.5 t, where the damage is simulated at ¼ span. When the corresponding vehicle weights are inferred using the rotations obtained from the inclinometer at the right-hand support (Figure 9 (d)) the error observed for this loaded truck peak is around 0.4 t. The

implication is that the method works best when two inclinometers are used to infer weights and hence to detect damage at any location along the length of the bridge.
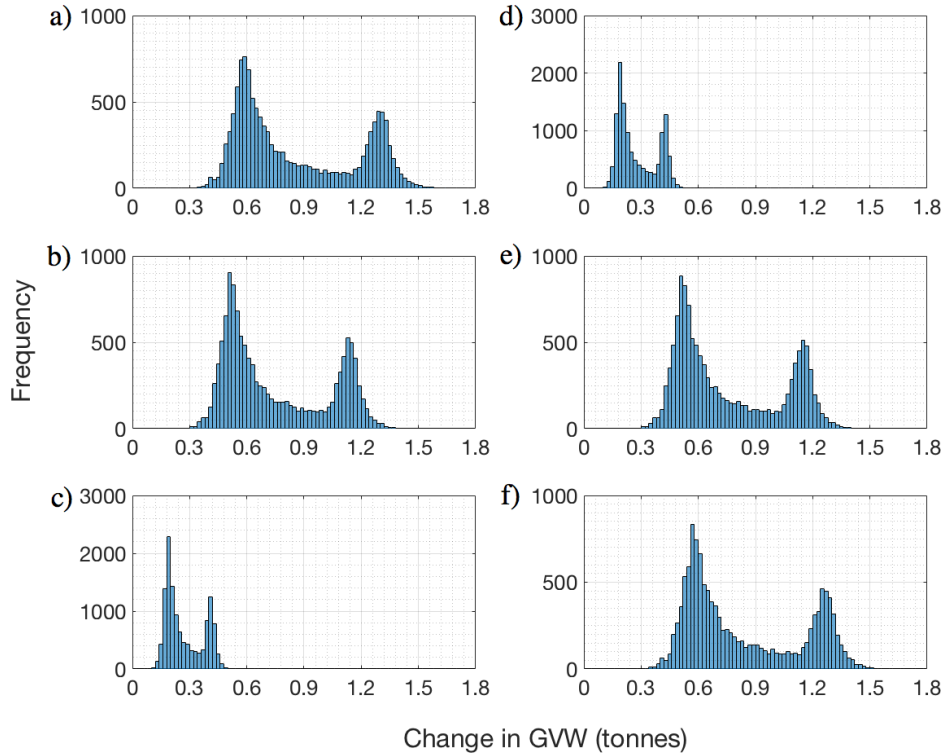

Figure 9. Histogram of change in GVW. Calculated using inclinometer placed at left-hand support while damage is modelled at a) ¼ L span b) ½ L span c) ¾ L span locations. Calculated using inclinometer placed at right-hand support while damage is modelled at d) ¼ L span e) ½ L span f) ¾ L span locations.

Having seen that the effect of damage on weight predictions is higher when the damage is closer to the sensor location, similar analyses presented in Figure 8 (c) are carried out for bridge damage at ¾ span where, this time, the average monthly tandem weights are calculated using the inclinometer placed at the right hand support (i.e. [20 m, 2.5 m]) and corresponding results are presented in Figure 10. While most of the ¾ span data for the damaged and healthy cases overlapped when the average monthly tandem weights were inferred using the inclinometer at the left-hand support (Figure 8(c)), it can be seen in Figure 10 that the results are considerably improved when data from the right hand

support are used. There are only two false positive results and one damage-missed case out of 48. It is therefore inferred that utilising inclinometers at two support locations makes it possible to identify damage occurring at any location along the length of the bridge structure using the proposed damage detection methodology.
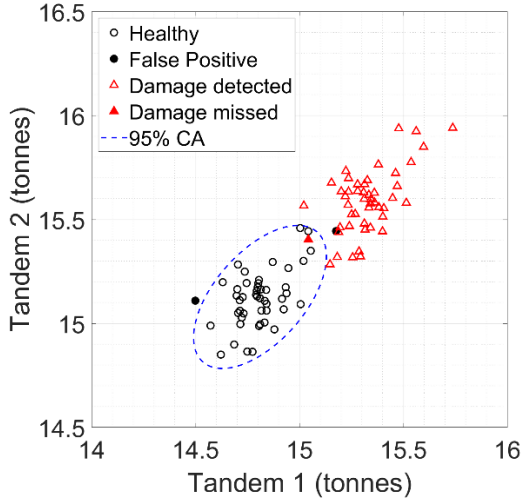

Figure 10. Monthly average tandem weights estimated using the inclinometer placed at right hand support when the damage is at ¾ L

It is acknowledged that measurements recorded in the field will contain a certain level of random error (noise) which needs to be considered while assessing the robustness of the proposed method. This is tested here by adding a noise vector, proposed by Zhu and Law [38]:

$$\{a\} = \{a_{calc}\} + E_p\{N\}\sigma \qquad (6)$$

where $\{a\}$ is a vector of corrupted rotations, $\{a_{calc}\}$ is a vector of noise-free rotations, E_p is the noise level$\{N\}$ is a standard normal distribution vector with zero mean and unit standard deviation and σ is the standard deviation of the noise-free rotations. Figure 11 shows a typical corrupted rotation time history corresponding to a 5 axle truck with 20% noise (i.e. E_p=0.2) at the scan frequency, i.e., all measurements randomly perturbed.
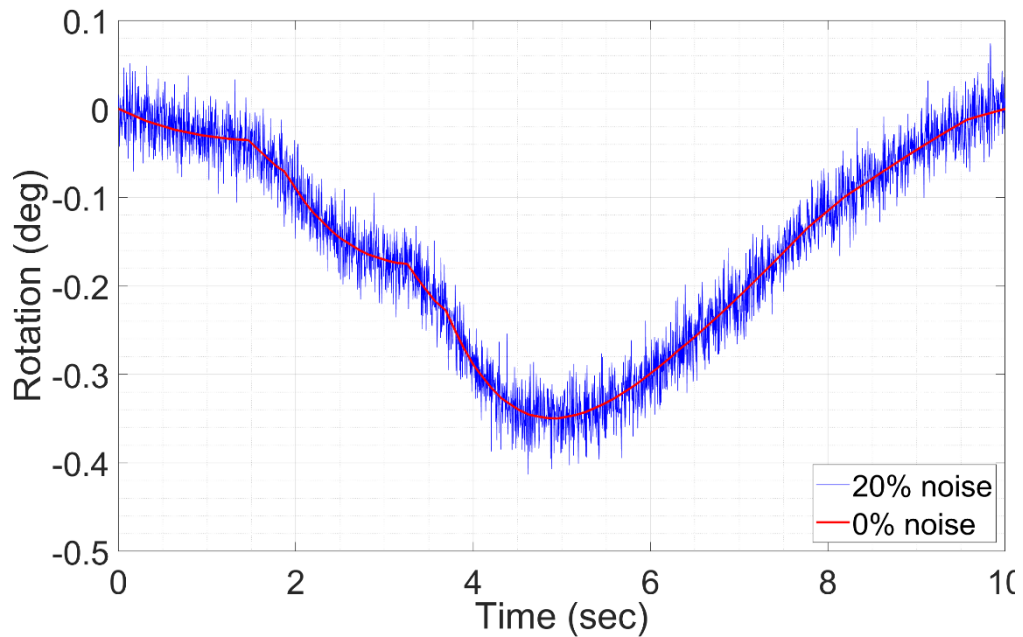
Figure 11. Noise free and corrupted rotation time history recorded using the left inclinometer for 20% noise level under 5 axle truck loading

The simulations are repeated with this added noise for each of two inclinometers placed, one at each support. While in the previous analyses, damage was simulated for all months (2009-2012) for which data was available, this time it is assumed that damage occurs at the start of the particular month of July 2012. For this case, the confidence area is derived using data collected between January 2009 and December 2011 (open black circles in Figure 12), well before the damage occurred. The figure also shows the average monthly tandem weights inferred using the rotation signals from January 2012 onward– some corrupted by damage which occurs in July 2012. When the damage is at the ¼ span location, the average tandem weights are inferred using the inclinometer at the left hand support (Figure 12 (a)). When the damage is at mid-span or ¾ L locations (Figure 12 (b) and (c)), the weights are calculated using the inclinometer at the right hand support. In practice where damage location is unknown, it is anticipated that data from both sensors would be analysed and any anomalous results would result in further

investigation. For all six months and all three possible damage locations, average monthly tandem weights between January and June 2012 (blue solid dots in Figure 12), fall inside the 95% confidence area, confirming that the bridge is healthy. Starting from July 2012 when the damage occurs at quarter and three-quarter span locations (i.e. Figures 12 (a) and (c)), the inferred average monthly tandem weights fall outside the confidence area, implying the existence of damage. For the damage scenario modelled at the midspan location, five inferred average monthly tandem weights fall outside the confidence area and one failing to identify the existence of damage. This is due to the damage locations being further away from the sensors; thus they have relatively less sensitivity to identify its presence.

It is noted that the algorithm proposed in this study requires very little computing power – it takes only seconds to predict the axle weights of a passing vehicle. Once the axle weights of the traffic population are known for some period (e.g. one month), generating a plot similar to Figure 12 does not require any intense data processing effort and could be done using simple software such as Excel, which is widely used among bridge owners/operators. The authors recommend the field validation of the methodology under more realistic conditions (measurement noise, temperature, etc.) in long term monitoring studies of full-scale bridges as a research area for future investigation. Overall, at this time, the results show that the proposed methodology is a promising tool for the condition assessment of bridges.
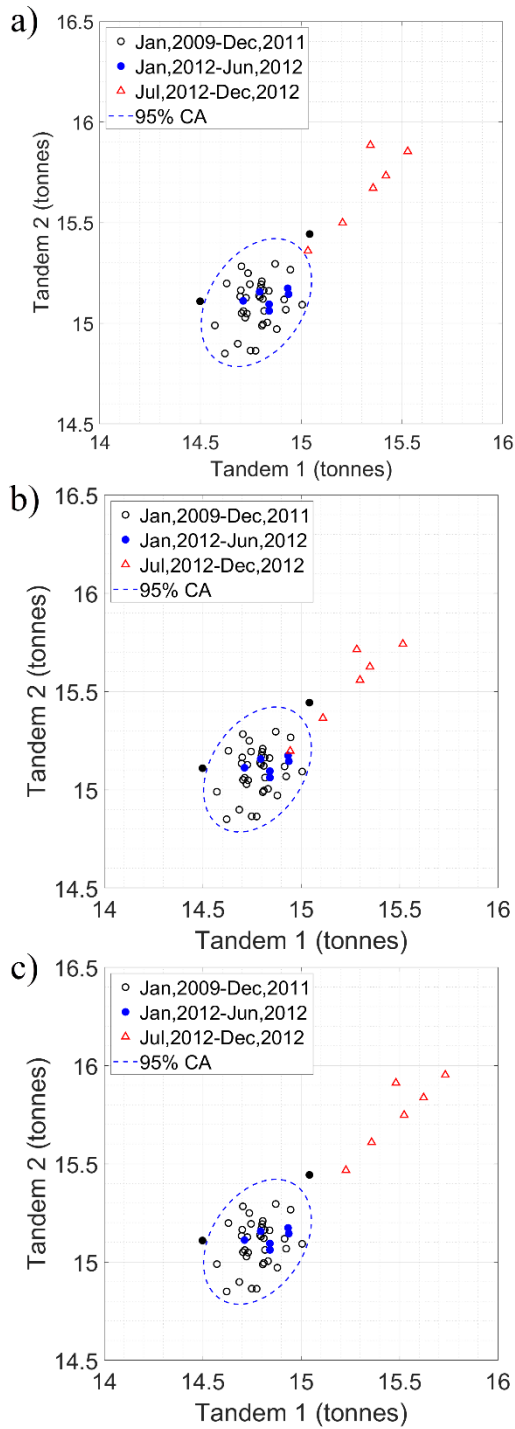
Figure 12. Monthly average tandem weights. a) estimated using the inclinometer placed at the left hand support when the damage is at ¼ *L*, estimated using the inclinometer placed at the right hand support when the b) damage is at ½ *L* and c) damage is at ¾ *L*. Damage is simulated from July 2012.

6   Conclusions

This paper presents a new bridge damage detection concept using information provided by a rotation-based Bridge Weigh-In-Motion system. It is shown that when damage occurs, a rotation based B-WIM system overestimates the weights of a passing vehicle. The inferred tandem weights in 5-axle (Class 9) vehicles are also affected and these errors can be exploited to detect damage. The statistical repeatability of traffic data is investigated using data from a WIM site with data over a 4-year period. It is concluded that:

- Rotation is a parameter that is sensitive to both local and global damage. Hence using a rotation based B-WIM system will give errors in weights which are damage sensitive. If there is a damage in the bridge, the system will generate errors in the weights of passing vehicles which can be used as indicators of damage.

- It is shown in this study that there is statistical repeatability in the tandem weights of Class 9 vehicles which can be used for bridge damage detection.

- The level of sensitivity of rotation to damage is related to the distance of the measurement from the location of damage. The effect of damage is higher for rotation measurements when the damage is closer to the sensor location. This issue is addressed by proposing two inclinometers, one at each end of the bridge.

- The method appears to be insensitive to measurement noise.

Acknowledgements

References

[1]   A. Žnidarič, V. Pakrashi, E. O'Brien, and A. O'Connor, "A review of road structure data in six European countries," *Proc. Inst. Civ. Eng. - Urban Des. Plan.*, vol. 164, no. 4, pp. 225–232, Dec. 2011, doi: 10.1680/udap.900054.

[2]   A. Rytter, "Vibration based inspection of civil engineering structures," Department of Building Technology and Structural Engineering, Aalborg University, Denmark, 1993.

[3]   a. J. Cardini and J. T. DeWolf, "Implementation of a Long-Term Bridge Weigh-In-Motion System for a Steel Girder Bridge in the Interstate Highway System," *J. Bridg. Eng.*, vol. 14, no. 6, pp. 418–423, 2009, doi: 10.1061/(ASCE)1084-0702(2009)14:6(418).

[4]   E. J. O'Brien, A. Znidaric, and A. T. Dempsey, "Comparison of two independently developed bridge weigh-in-motion systems," *Heavy Veh. Syst.*, vol. 6, no. 1, pp. 147–161, 1999, doi: 10.1504/ijhvs.1999.054503.

[5]   T. Ojio, C. H. Carey, E. J. OBrien, C. Doherty, and S. E. Taylor, "Contactless Bridge Weigh-in-Motion," *J. Bridg. Eng.*, vol. 21, no. 7, p. 04016032, Jul. 2016, doi: 10.1061/(ASCE)BE.1943-5592.0000776.

[6]   E. A. Oskoui, T. Taylor, and F. Ansari, "Method and sensor for monitoring weight of trucks in motion based on bridge girder end rotations," *Struct. Infrastruct. Eng.*, vol. 16, no. 3, pp. 481–494, Mar. 2020, doi: 10.1080/15732479.2019.1668436.

[7]   F. Moses, "Weigh-in-Motion System Using Instrumented Bridges," *Transp. Eng. J. ASCE*, vol. 105, no. 3, pp. 233–249, 1979.

[8]   A. Žnidarič, J. Kalin, M. Kreslin, P. Favai, and P. Kolakowski, "Railway bridge Weigh-in-Motion system," *Transp. Res. Procedia*, vol. 14, no. 14, pp. 4010–4019, 2016, doi: 10.1016/j.trpro.2016.05.498.

[9]   F. Marques, C. Moutinho, W.-H. Hu, Á. Cunha, and E. Caetano, "Weigh-in-motion implementation in an old metallic railway bridge," *Eng. Struct.*, vol. 123, pp. 15–29, Sep. 2016, doi: 10.1016/j.engstruct.2016.05.016.

[10]   A. Liljencrantz, R. Karoumi, and P. Olofsson, "Implementing bridge weigh-in-motion for railway traffic," *Comput. Struct.*, vol. 85, no. 1–2, pp. 80–88, 2007, doi: 10.1016/j.compstruc.2006.08.056.

[11]   A. O'Connor and E. J. O'Brien, "Traffic load modelling and factors influencing the accuracy of predicted extremes," *Can. J. Civ. Eng.*, vol. 32, no. 1, pp. 270–278, Feb. 2005, doi: 10.1139/l04-092.

[12]   A. Getachew and E. J. OBrien, "Simplified site-specific traffic load models for bridge assessment," *Struct. Infrastruct. Eng.*, vol. 3, no. 4, pp. 303–311, Dec. 2007, doi: 10.1080/15732470500424245.

[13]   A. González, P. Rattigan, E. J. OBrien, and C. Caprani, "Determination of bridge lifetime dynamic amplification factor using finite element analysis of critical loading scenarios," *Eng. Struct.*, vol. 30, no. 9, pp. 2330–2337, Sep. 2008, doi: 10.1016/j.engstruct.2008.01.017.

[14]   G. Yannis and C. Antoniou, "Integration of weigh-in-motion technologies in road infrastructure management," *ITE J. (Institute Transp. Eng.*, vol. 75, no. 1, pp. 39–43, 2005.

[15]   T.-L. Wang, C. Liu, D. Huang, and M. Shahawy, "Truck Loading and Fatigue

Damage Analysis for Girder Bridges Based on Weigh-in-Motion Data," *J. Bridg. Eng.*, vol. 10, no. February, pp. 12–20, 2005, doi: 10.1061/(ASCE)1084-0702(2005)10:1(12).

[16]   T. Guo, D. M. Frangopol, and Y. Chen, "Fatigue reliability assessment of steel bridge details integrating weigh-in-motion data and probabilistic finite element analysis," *Comput. Struct.*, vol. 112–113, pp. 245–257, 2012, doi: 10.1016/j.compstruc.2012.09.002.

[17]   D. Hajializadeh, E. J. OBrien, and A. J. O'Connor, "Virtual structural health monitoring and remaining life prediction of steel bridges," *Can. J. Civ. Eng.*, vol. 44, no. 4, pp. 264–273, Apr. 2017, doi: 10.1139/cjce-2016-0286.

[18]   D. Cantero and A. González, "Bridge Damage Detection Using Weigh-in-Motion Technology," *J. Bridg. Eng.*, no. 1, pp. 1–10, 2014, doi: 10.1061/(ASCE)BE.1943-5592.0000674.

[19]   D. Cantero, R. Karoumi, and A. González, "The Virtual Axle concept for detection of localised damage using Bridge Weigh-in-Motion data," *Eng. Struct.*, vol. 89, pp. 26–36, 2015, doi: 10.1016/j.engstruct.2015.02.001.

[20]   I. Gonzalez and R. Karoumi, "BWIM aided damage detection in bridges using machine learning," *J. Civ. Struct. Heal. Monit.*, vol. 5, no. 5, pp. 715–725, 2015, doi: 10.1007/s13349-015-0137-4.

[21]   E. OBrien, C. Carey, and J. Keenahan, "Bridge damage detection using ambient traffic and moving force identification," *Struct. Control Heal. Monit.*, vol. 22, no. 12, pp. 1396–1407, Dec. 2015, doi: 10.1002/stc.1749.

[22]   E. J. OBrien, M. J. Quilligan, and R. Karoumi, "Calculating an influence line

from direct measurements," in *Proceedings of the Institution of Civil Engineers - Bridge Engineering*, 2006, vol. 159, no. 1, pp. 31–34, doi: 10.1680/bren.2006.159.1.31.

[23] "Concast Precast Group Concrete Prestressed Girders Technical Guide." .

[24] C.-M. Wu and Y.-T. Chuang, "Roll angular displacement measurement system with microradian accuracy," *Sensors Actuators A Phys.*, vol. 116, no. 1, pp. 145–149, Oct. 2004, doi: 10.1016/j.sna.2004.04.005.

[25] Wyler AG, "Levelmatic 31 - High precision analog inclination sensor technical specification." 2016.

[26] D. G. Bruns, "An optically referenced inclinometer with sub-microradian repeatability," *Rev. Sci. Instrum.*, vol. 88, no. 11, p. 115111, Nov. 2017, doi: 10.1063/1.5010202.

[27] D. Inaudi and B. Glisic, "Interferometric inclinometer for structural monitoring," in *2002 15th Optical Fiber Sensors Conference Technical Digest. OFS 2002(Cat. No.02EX533)*, vol. 1, pp. 391–394, doi: 10.1109/OFS.2002.1000635.

[28] D. Hester, J. Brownjohn, F. Huseynov, E. Obrien, A. Gonzalez, and M. Casero, "Identifying damage in a bridge by analysing rotation response to a moving load," *Struct. Infrastruct. Eng.*, vol. 16, no. 7, pp. 1050–1065, Jul. 2020, doi: 10.1080/15732479.2019.1680710.

[29] D. Hester, J. M. W. Brownjohn, M. Bocian, and Y. Xu, "Low cost bridge load test: Calculating bridge displacement from acceleration for load assessment calculations," *Eng. Struct.*, vol. 143, pp. 358–374, Jul. 2017, doi: 10.1016/j.engstruct.2017.04.021.

[30] D. Hester, J. Brownjohn, M. Bocian, Y. Xu, and A. Quattrone, "Using inertial measurement units originally developed for biomechanics for modal testing of civil engineering structures," *Mech. Syst. Signal Process.*, vol. 104, pp. 776–798, May 2018, doi: 10.1016/J.YMSSP.2017.11.035.

[31] K. Faulkner, F. Huseynov, J. Brownjohn, and Y. Xu, "Deformation monitoring of a simply supported railway bridge under varying dynamic loads," 2018.

[32] K. Faulkner, J. M. W. Brownjohn, Y. Wang, and F. Huseynov, "Tracking bridge tilt behaviour using sensor fusion techniques," *J. Civ. Struct. Heal. Monit.*, no. 0123456789, Apr. 2020, doi: 10.1007/s13349-020-00400-9.

[33] F. Huseynov, C. Kim, E. J. OBrien, J. M. W. Brownjohn, D. Hester, and K. C. Chang, "Bridge damage detection using rotation measurements – Experimental validation," *Mech. Syst. Signal Process.*, vol. 135, p. 106380, Jan. 2020, doi: 10.1016/j.ymssp.2019.106380.

[34] K. Helmi, T. Taylor, A. Zarafshan, and F. Ansari, "Reference free method for real time monitoring of bridge deflections," *Eng. Struct.*, vol. 103, pp. 116–124, 2015, doi: 10.1016/j.engstruct.2015.09.002.

[35] D. Walker and D. Cebon, "The Metamorphosis of LTPP Traffic Data," 2012.

[36] C. Leahy, "Using Weigh-in-motion Data to Predict Extreme Traffic Loading on Bridges," University College Dublin, 2013.

[37] Federal Highway Administration, "Traffic Monitoring Guide," p. 462, Oct. 2016.

[38] X. Q. Zhu and S. S. Law, "Wavelet-based crack identification of bridge beam from operational deflection time history," *Int. J. Solids Struct.*, vol. 43, no. 7–8,